HHS Public Access

Author manuscript

Nat Biotechnol. Author manuscript; available in PMC 2016 July 01.

Published in final edited form as:

Nat Biotechnol. 2015 July ; 33(7): 730–732. doi:10.1038/nbt.3246.

Kinetic fingerprinting to identify and count single nucleic acids

Alexander Johnson-Buck[1,7,†], **Xin Su**[2,†], **Maria D. Giraldez**[3], **Meiping Zhao**[2], **Muneesh Tewari**[3,4,5,6], and **Nils G. Walter**[1,*]

[1]Single Molecule Analysis Group, Department of Chemistry, University of Michigan, Ann Arbor, Michigan, USA

[2]Beijing National Laboratory for Molecular Sciences, MOE Key Laboratory of Bioorganic Chemistry and Molecular Engineering, College of Chemistry and Molecular Engineering, Peking University, Beijing, China

[3]Department of Internal Medicine, Divisions of Hematology/Oncology and Molecular Medicine and Genetics, University of Michigan, Ann Arbor, Michigan, USA

[4]Department of Biomedical Engineering, University of Michigan, Ann Arbor, Michigan, USA

[5]Center for Computational Medicine and Bioinformatics, University of Michigan, Ann Arbor, Michigan, USA

[6]Biointerfaces Institute, University of Michigan, Ann Arbor, Michigan, USA

Abstract

MicroRNAs (miRNAs) have emerged as promising diagnostic biomarkers. We introduce a kinetic fingerprinting approach called Single Molecule Recognition through Equilibrium Poisson Sampling (SiMREPS) for the amplification-free counting of single unlabeled miRNA molecules, which circumvents thermodynamic limits of specificity and virtually eliminates false positives. We demonstrate high-confidence single-molecule detection of synthetic and endogenous miRNAs in both buffer and minimally treated biological liquids, as well as >500-fold discrimination between single nucleotide polymorphisms.

Stable, diagnostically useful miRNAs have recently been detected in blood and other body fluids, but reproducible quantification of circulating miRNAs has proven challenging[1]. Standard assays based on amplification by polymerase chain reaction (PCR), although highly sensitive, require time-consuming extraction and amplification steps. Next-generation sequencing approaches enable high-throughput profiling of RNA transcripts, but cannot reliably quantify low-abundance analytes (see Supplementary Note 1). Although a number of sensitive, amplification-free nucleic acid assays have been reported[2–5], these typically

*Corresponding author: nwalter@umich.edu.

[7]Current Address: Department of Cancer Biology, Dana-Farber Cancer Institute, Boston, Massachusetts, USA

†These authors contributed equally to this work.

Author contributions

N.G.W. and A.J.B. conceived the idea. A.J.B., N.G.W., and X.S. designed the experiments. X.S. and A.J.B. carried out experiments and analyzed the results. A.J.B., N.G.W., X.S., M.T., M.D.G., and M.Z. interpreted the results and wrote the paper.

Competing financial interests

The University of Michigan has filed a provisional patent (application serial number 14/589,467) on technologies described herein.

suffer from significant false positives and/or strict limits on target specificity imposed by the thermodynamics of hybridization[6] (see Supplementary Note 1).

Here we present a technique for the amplification-free single-molecule detection of unlabeled RNA biomarkers that circumvents many of the above issues. The approach, which we call Single-Molecule Recognition through Equilibrium Poisson Sampling (SiMREPS), is inspired by the super-resolution imaging technique DNA-PAINT[7] and exploits the direct binding of a short (9- to 10-nucleotide, nt) fluorescently labeled DNA probe to an unlabeled miRNA analyte immobilized on a glass surface (Fig. 1a). Using TIRF microscopy[8,9], both specific binding to the immobilized target and non-specific surface binding are detected (Supplementary Fig. 1). However, the equilibrium binding of the probe to the target yields a distinctive kinetic signature, or fingerprint, that can be used to achieve ultra-high discrimination against background binding (Fig. 1b,c). Because the kinetics of exchange for probes of ~6–12 nt are highly sensitive to the number of complementary bases between the probe and target[7,10,11], varying the length of the probe allows fine-tuning of the kinetic behavior to improve specificity of detection. For the probes used in this study, kinetics of binding and dissociation were found to be more closely correlated to probe length than to the melting temperature of the duplex (Supplementary Fig. 2).

As the transient binding of probes to an immobilized target can be idealized as a Poisson process, the standard deviation in the number of binding and dissociation events (N_{b+d}) is expected to increase only as $\sqrt{N_{b+d}}$, implying that the observation time can be lengthened to achieve arbitrarily high discrimination between target and off-target binding (see Supplementary Note 2). Consistent with this expectation, as the experimental acquisition time is increased, the signal and background peaks in histograms of N_{b+d} are progressively better resolved (Fig. 1d), and the width of the signal distribution increases only as $\sqrt{N_{b+d}}$ (Supplementary Fig. 3). Note that the choice of probe length is critical to achieve this separation on convenient experimental time scales (Supplementary Fig. 4).

To test the generality of SiMREPS, we evaluated four human miRNAs that are dysregulated in cancer and other diseases[12–14]: *hsa-let-7a*, *hsa-miR-21*, *hsa-miR-16*, and *hsa-miR-141*; and one non-human miRNA from *C. elegans: cel-miR-39* (Supplementary Fig. 5). Although the binding kinetics varied among the target-probe pairs, the signal and background peaks were well-separated for all targets (Supplementary Fig. 5b); by stipulating a threshold of $N_{b+d} \geq 15$, empirically perfect discrimination (specificity = 1) was achieved (Supplementary Fig. 5e). Standard curves constructed using this threshold for the five miRNAs show a linear dependence on target concentration over 2–3 orders of magnitude (Fig. 1e).

Because the lifetime of a short DNA duplex increases as an approximately exponential function of the number of base pairs[7,10,11], we reasoned that SiMREPS might be used to achieve excellent single-base discrimination. To test this hypothesis, we used a single fluorescent probe to discriminate between two *let-7* family members, *hsa-let-7a* and *hsa-let-7c*. We found that the lifetime of the probe-bound state τ_{on} differed by a factor of ~4.7 for the two targets, whereas the unbound-state lifetime τ_{off} showed no target dependence (Fig. 2a,b). Photobleaching is much slower than probe dissociation under our illumination

conditions (Supplementary Fig. 6). With the standard acquisition time of 10 min, *let-7a* and *let-7c* could be distinguished at the single-copy level with a discrimination factor > 100 at > 96% sensitivity, or with a discrimination factor > 570 (beyond the limit of quantification in this experiment) at ~70% sensitivity (Fig. 2b,c, Supplementary Fig. 7). Not only is this substantially larger than the typical discrimination factors of 2–100 reported for single mismatches using other hybridization-based probes[6,2,15,4], but as SiMREPS achieves discrimination at the single-molecule level, it is possible to independently quantify a target and a point mutant with high confidence in a mixture containing both species.

The high sensitivity and specificity of SiMREPS suggest that it may be capable of high-confidence RNA detection in complex biological matrices. To test this notion, we used SiMREPS to detect *hsa-let-7a* in HeLa whole-cell extract treated briefly with 1.67 % (w/v) SDS. The N_{b+d} histogram for endogenous *hsa-let-7a* showed a well-defined peak (Fig. 2d) similar to that observed for synthetic *hsa-let-7a* (Supplementary Fig. 5a) and *hsa-let-7c* (Supplementary Fig. 7) that vanished in the presence of an LNA *let-7* inhibitor designed to bind and sequester *let-7* family members. Notably, dwell time analysis of the fluorescent probe binding events yielded two populations of molecules that were readily resolved by *k*-means clustering of the τ_{on} values (Fig. 2e) and are consistent with the expected τ_{on} distributions for *hsa-let-7a* and *hsa-let-7c*.

To investigate whether SiMREPS can detect miRNAs of clinical interest in minimally treated biofluids, the assay for the prostate cancer biomarker *hsa-miR-141*[16] was conducted in a serum sample from a healthy individual after spiking in varying concentrations of synthetic *hsa-miR-141* together with 2% (w/v) SDS and 0.16 U/μL proteinase K to minimize degradation of the synthetic miRNA (Supplementary Fig. 8). The measured concentration (calibrated from the standard curve collected in buffer, Fig. 1e) was strongly correlated with the nominal spiked-in concentration (Fig. 2f, R > 0.999, slope = 1.07). Consistent with the expected low concentration (0.1–5 fM) of *miR-141* in the serum of healthy individuals[16], we measured a concentration of 0.4 ± 0.5 fM (*s.e.m.*, $n = 3$) in this serum specimen in the absence of spiked-in synthetic *miR-141*.

We have presented a method for the rapid, high-confidence, direct detection and quantification of specific nucleic acid biomarkers with transiently binding probes. SiMREPS lends itself to miniaturization, multiplexing and extension to non-TIRF-based detection approaches[17,18], so we expect it to find broad application in both clinical diagnostics and research.

Online Methods

Oligonucleotides

All miRNA samples were purchased from Integrated DNA Technologies with a 5′-phosphate modification and HPLC purification, except for *let-7a* and *let-7c*, which were purchased from Dharmacon with a 5′-phosphate modification, deprotected according to the supplier's instructions, and purified by reverse-phase C_{18} HPLC (Varian ProStar 210, Waters SunFire C18). All DNA probes were purchased from IDT and HPLC-purified by the manufacturer. LNA capture probes were purchased from Exiqon with HPLC purification.

Single-molecule fluorescence microscopy

SiMREPS experiments were performed using either a previously described prism-type TIRF microscope[19] (HeLa extract experiments) or a Olympus IX-81 objective-type TIRF microscope equipped with a 60× oil-immersion objective (APON 60XOTIRFM, 1.49NA) as well as Cell^TIRF and z-drift control modules (all other experiments). For prism-type TIRF experiments, fluidic sample cells were constructed using two pieces of double-sided tape sandwiched between a quartz slide and glass coverslip as previously described[19] (Supplementary Fig. 10a). For objective-type TIRF measurements, sample cells were constructed by fixing a cut 1-cm length of a pipet tip (Eppendorf) to a coverslip using epoxy adhesive (Double Bubble, Hardman Adhesives; Supplementary Fig. 10b). In either case, imaging surface (quartz slide or coverslip) was coated with a 1:10 mixture of biotin-PEG-5000 and mPEG-5000 (Laysan Bio, Inc.) immediately prior to construction of the sample cell as previously described[20]. Prepared slides were stored in the dark for up to two weeks.

SiMREPS quantification of synthetic miRNAs

Quantification of synthetic miRNA targets by SiMREPS was performed as follows. All miRNA handling was performed in GeneMate low-adhesion 1.7-mL microcentrifuge tubes, and dilutions for standard curves were performed in the presence of 0.03 mg/mL oligo(dT_{10}) (Integrated DNA Technologies) as a carrier. The slide surface was briefly incubated with T50 buffer (10 mM Tris-HCl, 1 mm EDTA, pH 8.0) followed by 1 mg/mL streptavidin. After 10 min, excess streptavidin was flushed out by 3 volumes of T50. The surface was then incubated with 20 nM of the appropriate biotinylated LNA capture probe (Exiqon, Inc.) in 1× PBS buffer for 10 min, and the excess flushed out by 3 volumes of 1× PBS. A 100-μL portion of target RNA (*hsa-let-7a*, *hsa-miR-16*, *hsa-miR-21*, *cel-miR-39*, or *hsa-miR-141*) was introduced into the sample chamber and incubated for 10 min (prism-type TIRF) or 60 min (objective-type TIRF). The longer incubation time for the objective-type TIRF measurements was necessary because of the tall (~1 cm) sample cell, which slowed the transport of analyte to the imaging surface. An imaging buffer containing 4× PBS, 2.5 mM 3,4-dihydroxybenzoate, 25 nM protocatechuate dioxygenase, 1 mM Trolox[21], and 25 nM of the Cy3- or Cy5-labeled fluorescent probe was added to the sample chamber. The transient binding of probes to captured target molecules was monitored for 10 min under illumination by 532 nm and/or 640 nm laser light. Image acquisition was performed at a rate of 2 Hz using an iCCD (iPentamax:HQ Gen III, Roper Scientific, MCP gain 70) for measurements of *let-7* in HeLa extract, and an EMCCD (IXon 897, Andor, EM gain 1000) for all other measurements.

Detection of endogenous *let-7* in crude HeLa extract

A 5-μL aliquot of HeLa whole cell extract (from Thermo Scientific In-Vitro Protein Expression Kit, # 88881) was incubated for 5 minutes at room temperature in the presence of 0 or 1.7% (w/v) sodium dodecyl sulfate (SDS) and 0 or 140 nM miRCURY *let-7* inhibitor (Exiqon). The lysate was vortexed, diluted 100-fold in 4× PBS imaging buffer containing 25 nM of the fluorescent probe for *hsa-let-7a*, and added to a microscope slide coated with an excess of the LNA capture probe. After a10-min incubation, the transient binding of the

fluorescent probe was observed by prism-type TIRF microscopy for 10 min as described above.

Detection of synthetic *miR-141* spiked into crude serum

50 uL of freshly thawed human serum (BioreclamationIVT, #BRH844152) was combined with SDS (final 2% w/v), proteinase K (New England BioLabs, Inc., P8107S; final concentration 0.16 units/μl), and synthetic *hsa-miR-141*, and incubated for 15 min at room temperature. Next, EDTA was added to a final concentration of 20 mM, and the sample heated to 90 °C in a copper bath for 2 min. After cooling to room temperature for 5 min, each sample was allowed to bind to the microscope coverslip surface for 1 h. Residual serum was removed, the surface washed with 1× PBS, and imaging carried out by objective-type TIRF microscopy as described above.

Analysis of SiMREPS data

Custom MATLAB code was used to identify sites of fluorescent probe binding and calculate intensity-versus-time trajectories from the CCD movie. Intensity trajectories were subjected to hidden Markov modeling (HMM) using QuB[22] in order to identify the number of binding and/or dissociation events (N_{b+d}) and mean dwell times in the bound (τ_{on}) and unbound (τ_{off}) states for each candidate molecule. Based on control measurements in absence of target, a threshold of $N_{b+d} = 15$ (6 standard deviations above background) was used to identify target molecules. Additional filtering criteria were used to reject spurious transitions detected by the HMM software: to be counted as a target molecule, a candidate must (1) have a mean bound-state intensity signal at least 2.5 standard deviations and 1000 counts above the mean background intensity, and (2) exhibit median values of τ_{on} and τ_{off} of at least 4 s. In the case of *let-7a* and *let-7c* discrimination, an intensity threshold of 500 counts was used instead, and criterion (2) was not applied since it would have eliminated a large fraction of *let-7c* molecules from analysis.

Kinetic Monte Carlo simulations of probe binding

SiMREPS probing of an immobilized target was simulated in MATLAB with the assumption of (pseudo-)first-order kinetics for both binding and dissociation. A random-number generator was used to make stochastic decisions as to whether a molecule will undergo a transition within discrete time steps of 0.5 s. The matrix of per-frame transition probabilities was generated from specified first-order rate constants. The number of transitions was recorded for each molecule for subsequent analysis.

PAGE assay of miRNA degradation in human serum

Synthetic miR-16 (final concentration 1 μM) was combined with sodium dodecyl sulfate (SDS, final concentration 0 or 2% w/v), proteinase K (New England Biolabs, final concentration 0, 0.08, 0.16, or 0.32 units/μL), and deionized water, then mixed with either PBS, pH 7.4 (final concentration 1×, Gibco) or human serum (final 50% v/v BioreclamationIVT) to a total volume of 20 μL. After 15 min incubation, samples were either left at room temperature or spiked with 2 μL EDTA (final concentration 20 mM) and heated to 90 °C for 2 min in a copper bath, then brought back to room temperature. Samples

were incubated for 1 h more at room temperature, then separated on a denaturing, 8 M urea, 20% (w/v) polyacrylamide gel. The gel was stained using SYBR gold (Life Technologies) and imaged on a Typhoon 9410 Variable Mode Imager (GE Healthcare Life Sciences).

Supplementary Material

Refer to Web version on PubMed Central for supplementary material.

Acknowledgments

This work was funded in part by the Department of Defense MURI Award W911NF-12-1-0420 (to N.G.W.) and US National Institutes of Health Transformative R01 grant R01DK085714 (to M.T.). X.S. acknowledges support from the China Scholarship Council. M.D.G. acknowledges initial support from a Rio Hortega Fellowship and later from a Martin Escudero Fellowship. The authors thank A. M. Chinnaiyan, M. Bitzer, A. Sahu, S. Pitchiaya, and L. A. Heinicke for helpful discussions.

References

1. Schwarzenbach H, Hoon DSB, Pantel K. Nat Rev Cancer. 2011; 11:426–437. [PubMed: 21562580]
2. Gunnarsson A, Jonsson P, Marie R, Tegenfeldt JO, Hook F. Nano Lett. 2008; 8:183–188. [PubMed: 18088151]
3. Geiss GK, et al. Nat Biotechnol. 2008; 26:317–325. [PubMed: 18278033]
4. Li L, Li X, Li L, Wang J, Jin W. Anal Chim Acta. 2011; 685:52–57. [PubMed: 21168551]
5. Ho SL, Chan HM, Ha AWY, Wong RNS, Li HW. Anal Chem. 2014; 86:9880–9886. [PubMed: 25207668]
6. Zhang DY, Chen SX, Yin P. Nat Chem. 2012; 4:208–214. [PubMed: 22354435]
7. Jungmann R, et al. Nano Lett. 2010; 10:4756–4761. [PubMed: 20957983]
8. Axelrod D, Burghardt TP, Thompson NL. Annu Rev Biophys Bioeng. 1984; 13:247–268. [PubMed: 6378070]
9. Walter NG, Huang CY, Manzo AJ, Sobhy MA. Nat Methods. 2008; 5:475–489. [PubMed: 18511916]
10. Cisse II, Kim H, Ha T. Nat Struct Mol Biol. 2012; 19:623–627. [PubMed: 22580558]
11. Dupuis NF, Holmstrom ED, Nesbitt DJ. Biophys J. 2013; 105:756–766. [PubMed: 23931323]
12. Lu M, et al. PLoS ONE. 2008; 3:e3420. [PubMed: 18923704]
13. Ruepp A, et al. Genome Biol. 2010; 11:R6. [PubMed: 20089154]
14. Russo F, et al. PLoS ONE. 2012; 7:e47786. [PubMed: 23094086]
15. Garcia-Schwarz G, Santiago JG. Angew Chem Int Ed. 2013; 52:11534–11537.
16. Mitchell PS, et al. Proc Natl Acad Sci U S A. 2008; 105:10513–10518. [PubMed: 18663219]
17. Sorgenfrei S, et al. Nat Nanotechnol. 2011; 6:126–132. [PubMed: 21258331]
18. Baaske MD, Foreman MR, Vollmer F. Nat Nanotechnol. 2014; 9:933–939. [PubMed: 25173831]
19. Michelotti N, de Silva C, Johnson-Buck AE, Manzo AJ, Walter NG. Methods Enzymol. 2010; 475:121–148. [PubMed: 20627156]
20. Abelson J, et al. Nat Struct Mol Biol. 2010; 17:504–512. [PubMed: 20305654]
21. Aitken CE, Marshall RA, Puglisi JD. Biophys J. 2008; 94:1826–1835. [PubMed: 17921203]
22. Nicolai C, Sachs F. Biophys Rev Lett. 2013; 08:191–211.

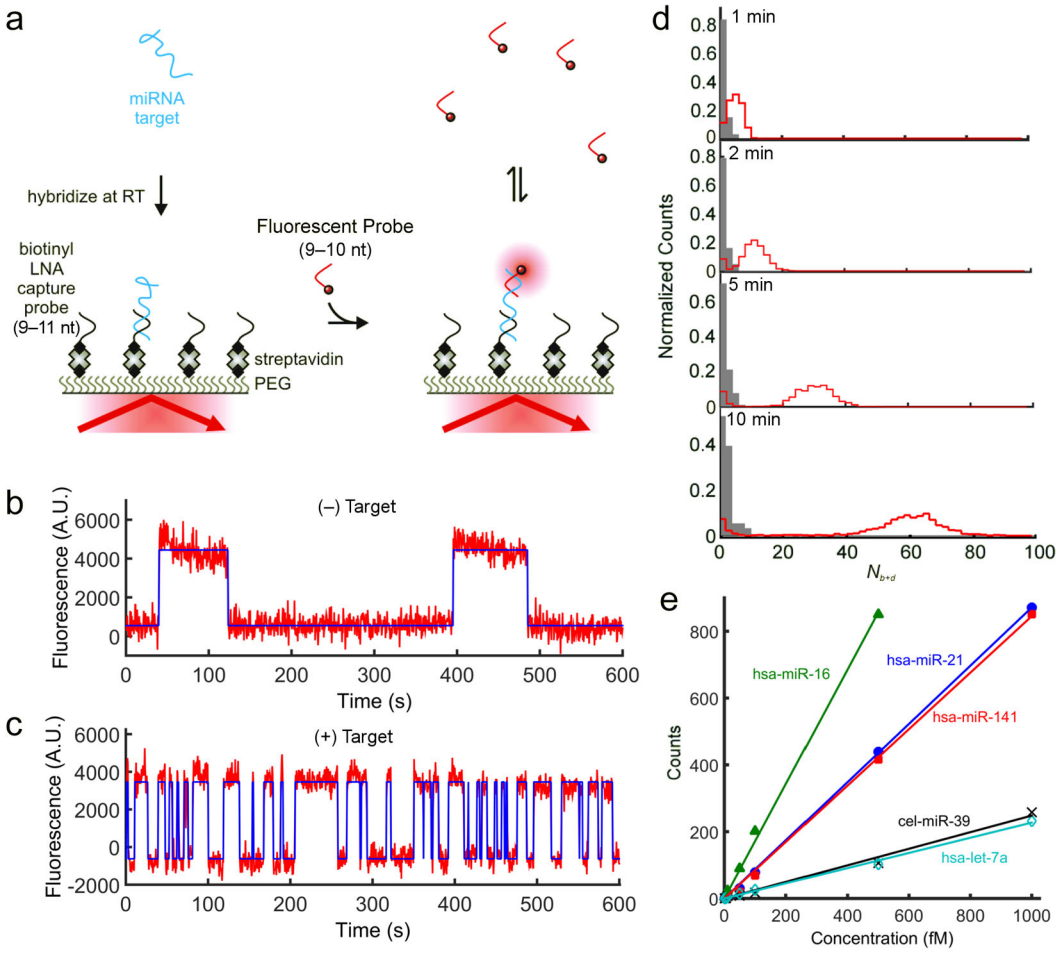

Figure 1. High-confidence detection of miRNAs with SiMREPS

a, Experimental approach of SiMREPS detection of miRNAs. An immobilized miRNA target is identified by fluorescence microscopy as the site of repeated transient binding by short fluorescent DNA probes. **b,c,** Binding of probes to the slide surface (**b**) exhibits kinetic behavior distinct from that of binding to a target molecule (**c**) (red curve = fluorescence intensity, blue curve = idealization from hidden Markov modeling). **d,** Histograms of the number of candidate molecules showing a given number of intensity transitions (N_{b+d}) in the absence (gray) or presence (red) of 1 pM *miR-141* with varying acquisition time. **e**, Standard curves from SiMREPS assays of five miRNAs. Linear fits were constrained to a *y*-intercept of 0, yielding R^2 values > 0.99.

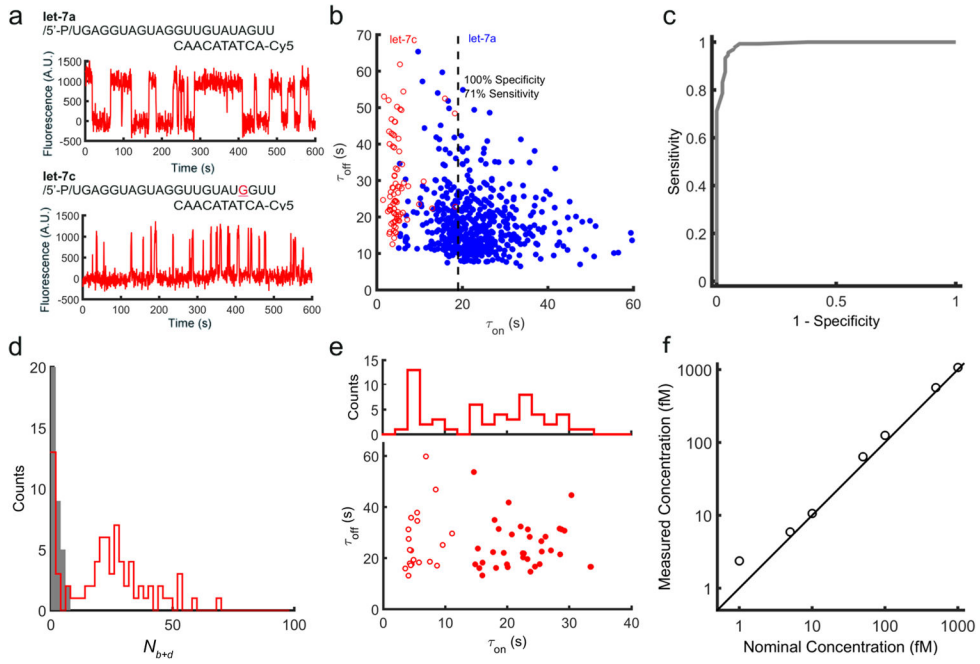

Figure 2. Single-molecule mismatch discrimination and detection of RNAs in crude biological matrices

a, The fluorescent probe for *let-7a* exhibits long lifetimes of binding to *let-7a* ($\boldsymbol{\tau_{on}}$ = 23.3 ± 8.3 s) but much more transient binding to *let-7c* ($\boldsymbol{\tau_{on}}$ = 4.7 ± 3.0 s) due to a single mismatch. **b,** Dwell time analysis enables high-confidence single-copy-level discrimination between *let-7a* and *let-7c*. **c,** Receiver operating characteristic (ROC) plot constructed by varying the $\boldsymbol{\tau_{on}}$ threshold for discriminating between *let-7a* and *let-7c*. **d,** $\boldsymbol{N_{b+d}}$ histogram for the detection of *let-7* in HeLa cell extract in the presence or absence of the miRCURY *let-7* inhibitor. **e,** Dwell times for molecules detected in HeLa extract using the fluorescent and capture probes for *let-7a*. The filled and open circles represent two clusters of target molecules classified by *k*-means clustering of $\boldsymbol{\tau_{on}}$ values. **f**, Quantification of synthetic *miR-141* spiked into human serum together with proteinase K and SDS.